Journal of ELECTRICAL ENGINEERING, VOL 51, NO 1-2, 2000, 30–35

TECHNOLOGY AND PERFORMANCE OF X– AND γ–RAY 32 PIXEL LINE DETECTOR BASED ON SEMI–INSULATING GaAs

František Dubecký et al *

Technology, electrical characteristics and detection performance of a recently developed and fabricated 32-pixel line array chip for detection of X- and γ-rays named "SAMO" based on semi-insulating GaAs are reported. The chip with dimensions of $7 \times 2.4 \times 0.2\,\mathrm{mm}^3$ is mounted onto a ceramic holder. A single pixel has an active area of $2000 \times (120 \div 180)\,\mu\mathrm{m}^2$ with a pitch of $220\,\mu$m. Current density (300 K) of a single pixel at a bias voltage of 125 V ranges between $9 \div 50\,\mathrm{nA/mm}^2$. The threshold voltage ranges between $150 \div 500$ V. Pulse-height spectra in both the side as well as the top irradiation modes measured using 59.5 keV and 122 keV γ-sources are demonstrated. The best detection performance observed with SAMO pixel line detector for detection of 122 keV gamma rays at 300 K in the side irradiation reached a charge collection efficiency 85 %, relative energy resolution in HWHM 4 %, and detection efficiency in the photopeak 50 %.

K e y w o r d s: radiation detector, semiconductor, GaAs, semi-insulating, pixel line

1 INTRODUCTION

Semiconductor X- and γ-ray detector is the key element for digital radiology systems of a new generation. The most attractive applications (*eg* on-line process control, security, medicine) need detectors operated at room temperature (RT) based on wide band-gap (> 1.2 eV) compounds where at least one of the constituents has an atomic number Z larger than 30 [1]. A further important requirement for detector includes a good enough relative energy resolution which is for 60 keV photons a value $< 12\,\%$ in HWHM (half width at half maximum). This requirement follows from the recently developed "dual X-ray" image mode [2] giving directly a digital image of the object density (or Z using corresponding calibration) and allows selection of a "soft" or a "hard" part from the integral digital image. Such an image mode needs a satisfactorily fine energy separation of the detected photons *eg* from the broad energy spectrum of an X-ray tube source [3]. Development and final effective fabrication of a monolithic detector array based on a suitable semiconductor is the most important task of the present period. Figure 1 presents the stopping power of the most widely used semiconductor materials for fabrication of X- and γ-ray detectors in terms of their attenuation. This parameter is given for material thickness from $50\,\mu$m up to 5 mm for three photon energies 30, 60, and 122 keV. The attenuation A was calculated as the ratio

$$A = \frac{n}{n_0}\,,$$

where n_0 is the number of incident photons per unit area, and n is the number of stopped photons. Both quantities relate each other via equation

$$n = n_0 e^{-\mu x}$$

or

$$n = n_0 e^{-\frac{\mu}{\rho}(\rho x)}$$

where μ is the linear attenuation coefficient (in cm^{-1}), x is the thickness of material, and μ/ρ is the mass attenuation coefficient (in $\mathrm{g\,cm}^{-2}$) where ρ is the mass density (in $\mathrm{g\,cm}^{-3}$). There are three basic mechanisms contributing to the absorption of the photon energy: (i) photoelectric effect, (ii) Compton scattering and (iii) pair production. In our calculation of the stopping power we neglected the last mechanisms due to the energy range of interest. The values of coefficients for a particular atom and a given energy of photons corresponding to each mechanism mentioned were taken from [4]. Total attenuation coefficients

* Frantiek Dubeck (elekfdub@savba.sk), Juraj Darmo, Marin Krempask, Mria Sekov, Bohumr Zako, Pavol Bohek, Igor Bee, Miloslav Ruek, Institute of Electrical Engineering, Slovak Academy of Sciences, Dbravsk cesta 9, SK-84 239 Bratislava 4, Slovakia

Vladimr Neas, Faculty of Electrical Engineering and Information Technology, Slovak University of Technology, Ilkoviova 3, SK-812 19 Bratislava 1, Slovakia

Pier G. Pelfer, University of Florence and INFN, Largo E. Fermi 2, Firenze, I-50125 Italy

Rudolf Senderk, Emil Pink, Institute of Physics, Slovak Academy of Sciences, Dbravsk cesta 9, SK-842 28 Bratislava 4, Slovakia

Milo Somora, Frantiek Kolesr, Faculty of Electrical Engineering and Informatics, Technical University, Park Komenskho 2, SK-043 89 Koice, Slovakia

Peter Hudek, Ivan Kosti, Institute of Informatics, Slovak Academy of Sciences, Dbravsk cesta 9, SK-828 39 Bratislava, Slovakia

ISSN 1335-3632

Table 1. Selected information and physical parameters (measured at room temperature) of the used semi-insulating materials. Both wafers have crystallographic orientation ⟨100⟩.

Material label:	A1	A2
Producer	AXT	AXT
Growth method	VGF	VGF
EPD, cm^{-2}	5×10^3	$< 3 \times 10^3$
Resistivity, Ωcm	8.8×10^7	4.6×10^7
Hall mobility, cm^2/Vs	4.4×10^3	6.2×10^3

were then calculated by a weighing sum for all atoms included in the compound according to the expression

$$\frac{\mu}{\rho} = \sum_k \frac{\mu_k}{\rho_k} a_k \,,$$

where a_k is the mass fraction of the k-th element of the compound. In Fig. 1, a comparison of the attenuation ability of GaAs, InP, CdTe and ZnCdTe is presented. For each semiconductor material, the attenuation curves for photons with energy 30, 60 and 122 keV are shown. The attenuation curve for photons with energy from the range 30–122 keV lies in the area between these two curves. From Fig. 1, it is clearly visible that for lower energies of photons the materials do not exhibit large differences in the stopping power (see *eg* CdTe and InP), while for higher energies of photons this effect becomes significant.

The use of GaAs as the base material for detectors operated at RT presents the best choice from the economical, as well as the technical points of view (see *eg* [5–11] and references therein). Moreover, a multipixel detector array in the form of a line chip presents the basic element for a longer X- and γ-ray detection line or a scanner that offer the lowest cost and fastest way to reach the goal: digital radiology instrumentation. Further, the detector line allows its application in both the "top" or "side" irradiation mode, when incident photons are in parallel or perpendicular to the internal electric field direction, respectively. The side irradiation mode presents a simple possibility to reach a very long stopping length for photons even if a relatively thin detector structure is used.

We report for the first time on electrical characteristics and detection performance of a recently developed and fabricated 32-pixel line chip based on semi-insulating (SI) GaAs named "SAMO" using a Schottky barrier active electrode system. The chip technology was verified using two various SI GaAs wafers with a thickness of 200 μm. The active area of a pixel is $2000 \times (120 \div 180)\ \mu m^2$. With the pitch of 220 μm between pixels, a spatial resolution better than 200 μm (at about 70 μm after precise digital processing) could be achieved.

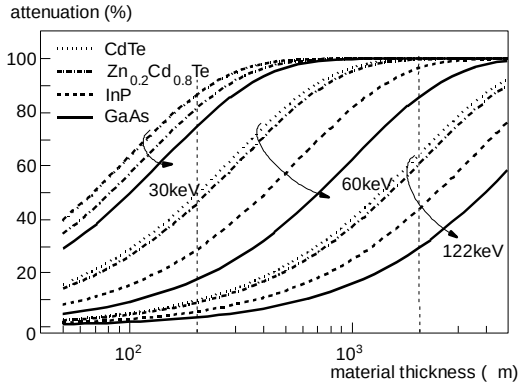

Fig 1 Calculated attenuation coefficient vs. material thickness (50 μm−5 mm) for four semiconductors most widely used for X-ray detector fabrication.

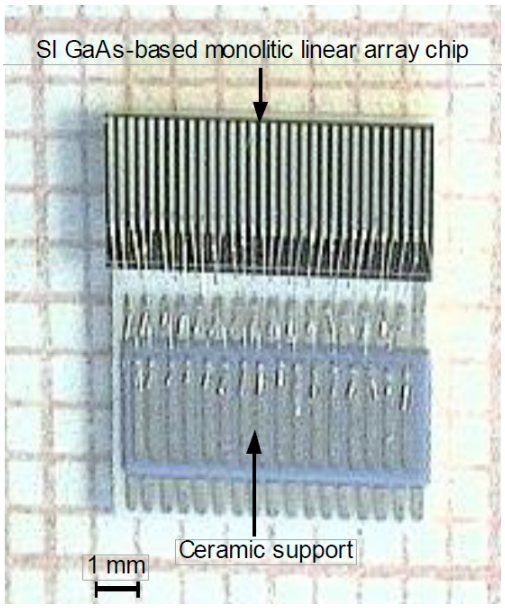

Fig 2 Picture of the SAMO chip mounted onto a ceramic support.

2 TECHNOLOGY

Detectors were fabricated from two initially undoped SI GaAs substrates fabricated by AXT (American Xtal Technology) grown by VGF (vertical gradient freeze) hereafter labelled A1 and A2. Basic physical parameters of materials used are summarised in Table 1. The substrates were polished from both sides to a final thickness of 200 μm. A silicone nitride passivation layer with a thickness of 100 nm was sputtered onto the freshly etched GaAs surfaces. Windows for active electrodes were opened in the passivation layer by dry etching in the O_2 plasma. Further, detectors were symmetrically processed using both-sided photolithography. The active electrode consists of a Schottky barrier formed by Ti/Pt/Au metallization (total thickness of 120 nm) using the lift-off technique. The back contact was formed by evaporation of a non-alloyed Au/Ge/Ni multilayer producing an "ohmic"

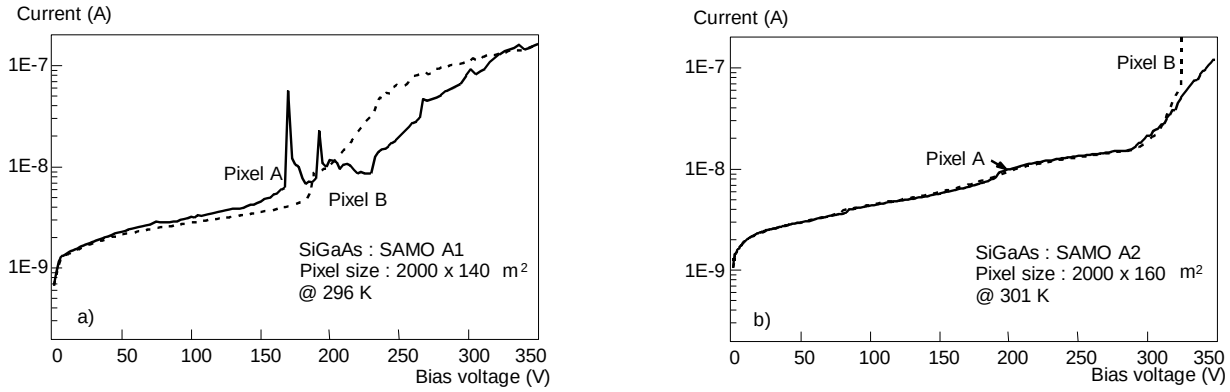

Fig 3 Room-temperature I-V characteristics of two pixels of SAMO chips fabricated from two various SI GaAs substrates (A1, A2) produced by AXT.

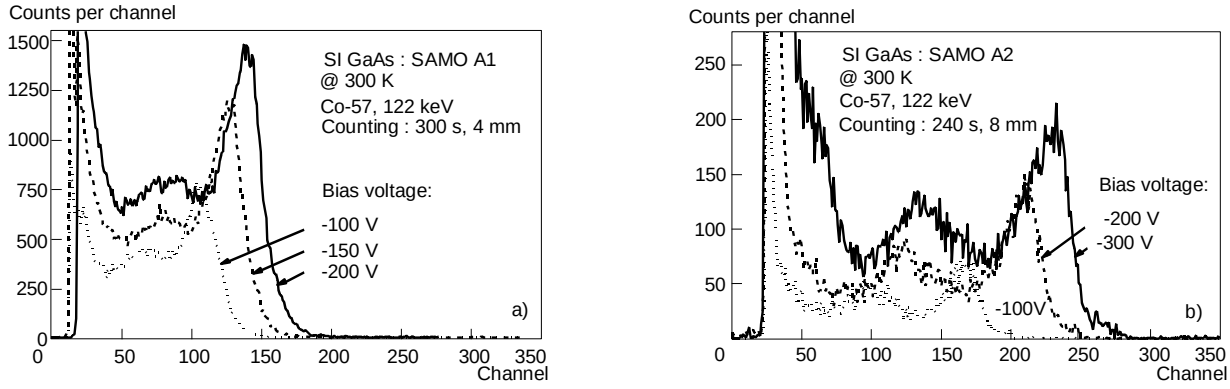

Fig 4 Pulse-height spectra of Co-57 source (122 keV) detected by SAMO detectors fabricated from the two substrates (A1, A2) measured at 3 various bias voltages (RT).

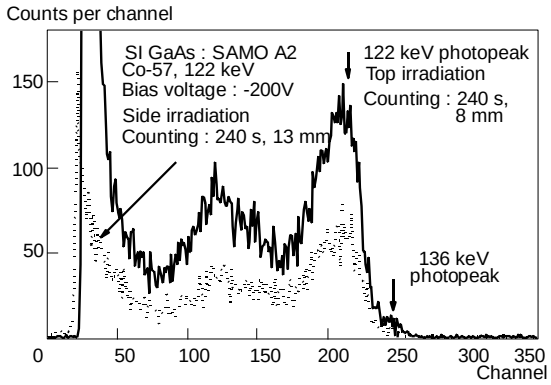

Fig 5 Pulse-height spectra of a Co-57 source (122 keV) detected by the SAMO A2 chip at a bias voltage of -200 V (RT) in the *top* (full) and *side* (dot) irradiation modes.

contact. In the case of the A2 structure, an originally developed "buffer" was deposited using implantation in combination with diffusion [12] prior to evaporation of the metal electrode. Finally, the chip was glued on a ceramic holder by a silver epoxyresin. Individual pixels were contacted by ultrasonic bonding using an Al wire bonded directly onto active pixels, without extra bonding pads. Figure 2 shows a picture of the chip with dimensions of $7\times2.4\times0.2\,\mathrm{mm}^3$ mounted on the ceramic holder. A single step micro-Peltier cooler and IC temperature transducer (AD590) for temperature control and stabilisation is currently assembled from the back of the ceramic holder. The chip is applicable in both *top* and *side* irradiation modes allowing two combinations of stopping length and spatial resolution: $200\,\mu$m & $(120–180)\times2000\,\mu\mathrm{m}^2$ (the top mode) or $2000\,\mu$m & $200\times(120–180)\mu\mathrm{m}^2$ (the side irradiation mode), respectively.

3 DETECTOR TESTING

Current-Voltage characteristics of two selected chip pixels measured at room temperature (296–301 K) for the two used SI GaAs materials are presented in Fig. 3. The current per pixel at a bias voltage of 100 V was $3(+/-0.5)$ nA, and $11(+/-2)$ nA for the chips fabricated from material A1, and A2, respectively. These values correspond to a current density of about 9 to $50\,\mathrm{nA/mm}^2$, respectively. The threshold voltage of pixels ranged between 150–200 V for A1, and 300–500 V for A2 sample.

Pulse-height spectra measured in the top irradiation mode using ^{57}Co source (peak 122 keV) detected by SI GaAs pixel detectors at three various bias voltages are illustrated in Fig. 4. A comparison of the *top* and *side* irradiation modes for the same radiation source at a bias

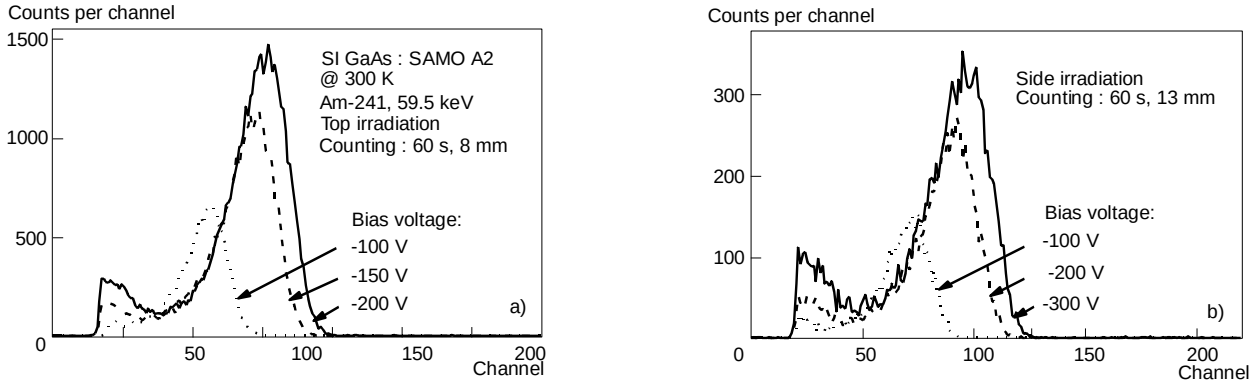

Fig 6 Pulse-height spectra of an Am-241 source (59.5 keV) detected by the SAMO chip A2 at three various bias voltages (RT) in the *top* (a) and in the *side* (b) irradiation modes.

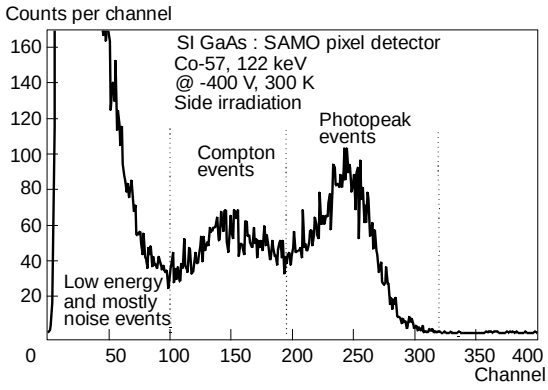

Fig 7 Pulse-height spectra of a SI GaAs SAMO pixel detector with demonstration of interesting interaction regions used for the calculation of the detection efficiency — DE.

Table 2. Summary of the observed electrical characteristics and detection performances (122 keV, RT) of the SAMO X- and γ-ray detectors based on semi-insulating GaAs.

Detector series label:	A1	A2
Saturation dc current (bias 125 V), nA	3 ± 1	14 ± 3
Threshold voltage*, V	210	500
CCE*, %	50	85
HWHM**, %	9.5	4
Peak to valley ratio*	2/1	3.5/1

* Maximum observed value
** Minimum observed value

voltage of -200 V is illustrated in Fig. 5. In Fig. 6, pulse-height spectra using ^{241}Am source (59.5 keV) for both, the top (a) and the side (b) irradiation modes are demonstrated. The samples were measured at room temperature in darkness in the voltage range of 80–500 V. Detection performance of the detector was tested using a standard front-end (F-E) electronic chain consisting of a charge sensitive preamplifier (Canberra Model 2003 BT), shaping amplifier (EG&G, ORTEC Model 572), analog-to-digital converter (EG&G, ORTEC Model 800) and a multichannel analyser. The time constant of the shaping amplifier was set to $0.5\,\mu$s. Electronic noise of the used F-E chain tested by a pulsar presents 15 channels HWHM. Bias voltage polarity on the irradiated pixel was negative, *ie* the top of the detector.

Estimation of the detection efficiency of the tested detectors was performed by using a radiation source ^{57}Co emitting mostly γ-photons with energy of 122 keV. The number of incident γ-photons to the detector pixel with area S was determined from the known duration of irradiation t, activity of radiation source A, and its distance y from the detector according to the relation

$$I = A\frac{S}{4\pi y^2}t\,.$$

The activity of the radiation source was 1.02×10^7 Bq (here, the decay period of the ^{57}Co source 269.8 days was taken into account). Dimensions of the tested pixel detector were: thickness 0.2 mm, length 2 mm, and width 0.16 mm. The distance between the detector and the radiation source was 8 mm for the *top* irradiation and 13 mm for the *side* irradiation. The collection time was 240 s. The number of incident γ-photons calculated form measured photon counts $I_T = 9.7 \times 10^5$, and $I_S = 3.7 \times 10^4$ was observed for the *top* and *side* irradiation, respectively. Detection efficiency — DE calculated from detector thickness and atomic number of GaAs material was $p_T = 3.4\,\%$, and $p_S = 29\,\%$ for the *top* and *side* irradiation, respectively. The number of γ-photons that interact within the detector pixel during 240 s therefore is:

$$U = Ip\,.$$

For the *top* irradiation, $U_T = 3.3 \times 10^4$ and for the *side* irradiation, $U_S = 1.1 \times 10^4$. Two values of a relative quantity of events registered by the detector pixel in terms of DE were estimated: DE in the photopeak and the total DE including photopeak and Compton events. Figure 7 shows a typical spectrum of a detector pixel using the ^{57}Co radiation source with demonstration of the two selected energy regions of interesting interactions. The estimated values of DE at different bias voltages for both the *top* and *side* irradiation modes are demonstrated in Fig. 8.

4 DISCUSSION

Two dashed lines drawn in Fig. 1. correspond to the stopping length of SAMO single pixel: (i) 200 μm for the *top* mode, and (ii) 2000 μm for the *side* mode. It is clearly seen in the figure that the calculated attenuation for photon energy ≤ 30 keV in the *top* mode is higher than 74 %. On the other hand, attenuation in the *side* mode presents a value of about 85 % for the photon energy of 60 keV. These values confirm the applicability of a GaAs detector in the considered energy regions including *eg* digital mammography application even in the *top* mode where the optimum photon energy is about 18 keV (see [8] and references therein) or medical image in general using the *side* mode, *ie* a long stopping length. The most important advantage of the line detector array is a possibility of the detector to operate in the *side* irradiation operation mode. This is impossible to use in the case of a full area pixel detector (*eg* presently developed array of 125×125 pixel array with 150 μm pitch within the EC project MEDIPIX).

The obtained difference in the current density (Fig. 3) is explicable by the different quality of used substrates, including impurity, defect density, structural and space charge inhomogeneities [13], and finally, the particular electrode technology applied. The used substrates were grown by the VGF method which is known to yield low dislocation density materials (etch pitch density, EPD $< 10^4 \mathrm{cm}^{-3}$). From a comparison of the basic physical characteristics (mainly the Hall mobility and dislocation density) of the two SI GaAs wafers used for SAMO chip fabrication (Table 1), it can be concluded that material labelled A2 shows better quality. Also, as we observed from a detail material analysis [13], A2 has a lower content of chemical impurities, mainly metals (Cu, Fe, Ti) creating deep acceptor-like levels in the material and space-charge inhomogeneities. These defects lower the carrier lifetime, which results in higher trapping, *ie* lowering of the CCE of a radiation detector. The evaluated difference in material quality correlates with the measured I–V characteristics and detection performance, in particular the lower values of the saturation current and estimated CCE of A1 detector are related to a higher trapping.

The best performance observed (at RT) for SI GaAs-based SAMO pixel detector present: (i) charge collection efficiency — CCE 85 %, (ii) HWHM 5.5 % (122 keV) and 12 % (59.5 keV) including the electronic noise of redaout chain, (iii) detection efficiency — DE in photopeak 50 % (from the theoretical value), and (iv) peak to valley — P/V ratio 3.5 (122 keV) and 15 (59.5 keV). The observed energy resolution was improved to a value of about 4 % and 9 % HWHM at 122 keV and 59.5 keV, respectively, after the electronic noise extraction from the spectra. The CCE, signal to noise and P/V ratio increases with the increasing bias up to a threshold voltage according to expectation. The observed electrical characteristics and determined parameters of tested detectors are summarised in Table 2. Better detection parameters were observed with A2 sample having the highest value of the threshold voltage (Fig. 3b). This is explainable by a larger distance of the saw cutting trace from the pixel edges (at about 100 μm) and by the influence of the buffer layer placed between the wafer and the back metallization.

The sample A2 pulse height spectra observed for the *top* and *side* irradiation modes are demonstrated in Fig. 5 (122 keV) and Fig. 6 (59.5 keV). The estimated counting rate in terms of DE for a pixel is higher for the *side* irradiation mode due to about 10 times longer stopping length (note that the results presented in Fig. 5 and Fig. 6 were obtained at a larger distance of the radiation source from the detector in the *side* irradiation mode). As it follows from the results, A2 sample gives a better DE in the side irradiation mode, 98 % and 50 % for the total and photopeak DE, respectively. Sample A1 shows nearly the same dependence of DE vs. bias until a breakdown voltage (about 200 V) as follows from Fig. 8. Such a low value of the breakdown voltage can be explained by placing the cutting saw trace at a very short distance from the pixel edges (at about 25 μm). Moreover, in A1 technology, no buffer layer was placed under the back metallization. From Fig. 8 it can be concluded that the value of the threshold voltage is of key importance due to the control of the distribution of the electric field inside the detector, *ie* its actual active volume.

It summarised from our study that the most critical points of the technology include the "buffer" layer placed between the substrate and metallization of the back electrode [12], and cutting or cleaving a wafer into single chips. The distance of the cutting saw trace from the face of pixels plays a key role in control of the surface leakage current, as well as the threshold voltage. The most critical situation is for the two edge pixels in the line.

The shape of the photopeak as well as low noise observed prove the good performance of the developed SI GaAs-based pixel detectors and their applicability in X- and γ-ray digital radiology systems of a new generation. Compatibility of the SAMO monolithic linear array with a multichannel readout chip (XRD-TO1) based on C-MOS technology [14] is presently being tested for detection performance. The readout chip accepts dc coupling of a single pixel with the channel input up to about 50 nA dc current. Preliminary results are promising and will be published elsewhere.

5 CONCLUSIONS

The technology of a new device — semiconductor sensor consisting of a monolithic 32-pixel linear array based on bulk SI GaAs applicable for the detection of X- and γ-rays — was developed. Electrical characteristics and detection performance of radiation detectors fabricated from 2 various standard quality bulk GaAs materials using Co-57 and Am-241 photon sources were demonstrated. The promising results obtained confirm the applicability of SI GaAs-based radiation detectors in the field of digital radiology. The developed technology presents

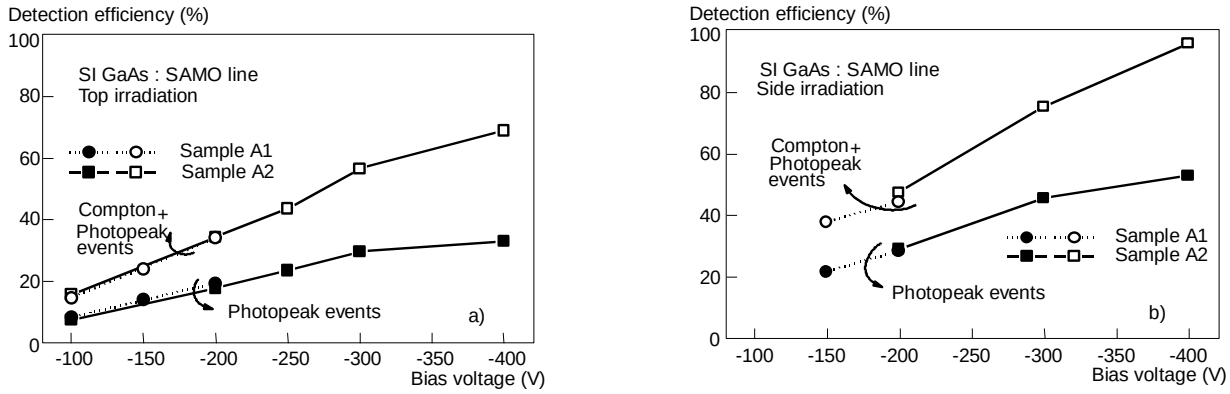

Fig 8 The dependence of the estimated detection efficiency at various bias voltages for SAMO pixel detectors in the *top* (a) and the *side* (b) irradiation modes.

the simplest and lowest cost processing that could finally be used for small or medium scale production, after optimisation of a few resting critical steps is achieved.

Acknowledgement

The work was supported in a part by grant of the Slovak Grant Agency for Science No. 2/5166/99 and of the Slovak Ministry of Economy.

References

[1] TOVE, P. A.: Sensors and Actuators **5** (1984), 103.

[2] HARRISON, R. M.: NIM **A 310** (1991), 24.

[3] CADEDDU, S.—CALIGIORE, C.—CARIA, M.—LAI, A.—LOI, S.—Lo PRESTI, D.—PANEBIANCO, S.—PETTA, C.—PORCU, P.—RANDAZZO, N.—RANDACCIO, P.—REITO, S.—RUSSO, G. V.: Physica Medica **vol. XIV** Supplement 2 (1998), 23.

[4] McMASTER, W. H-N. K.—DelGRANDE, N. K.—MALLETT, J. H.—HUBBELL, J. H.: Compilation of X-Ray Cross Sections (Lawrence Livermore Lab., Livermore 1969).

[5] SCHLESSINGER, T. E.—JAMES, R. B.: Semiconductors for Room Temperature Nuclear Detector Applications, Semiconductors and Semimetals, 43, treatise eds. Willardson, R.K., Beer, A.C., and Weber, E.R., (Academic Press, San Diego 1995).

[6] Properties of GaAs, 3rd Edition, eds. Brozel, M.R., and Stillman, G.E., EMIS Datareview, Ser. No. 16, INSPEC IEE, London 1996, p. 942.

[7] TEMPLER, R. H.—BERTOLUCCI, E.—BOTTIGLI, U.—Del GUERRA, A.—MESSINEO, A.—NELSON, W. R.—RANDACCION, P.—ROSSO, V.—RUSSO, P.—STEFANINI, A.: NIM **A 310** (1991), 210.

[8] Physica Medica **XIV** Supplement 2 (1998), 1–33.

[9] Proc. of 5th International Workshop on GaAs and Related Compounds, Udine 1998, published in NIM **A 410** (1999), 1–132.

[10] DUBECKÝ, F.—DARMO, J.—HLAVÁČ, S. BENOVIČ, M. PIKNA, M.—PELFER, P. G.—FÖRSTER, A. KORDOŠ, P.: NIM **A 377** (1996), 475.

[11] DUBECKÝ, F.—KREMPASKÝM.—PELFER, P. G.—DARMO, J.—PIKNA, M.—ŠATKA, A.—SEKÁČOVÁ, M.—RUŽEK, M.: Nuclear Phys. (Proc. Suppl.) **54B** (1997), 368.

[12] DUBECKÝ, F.—DARMO, J.—PELFER, P. G.: Patent pending.

[13] DUBECKÝ, F.—DARMO, J.—KREMPASKÝM.—NEČAS, V.—PELFER, P. G.—BOHÁČEK, P. Sekáčová,—M.: Proc. of the 1998 IEEE Semiconducting and Insulating Materials Conference, SIMC-X, Berkeley 1998, eds. Z.L. Weber, C.J. Miner, IEEE Publ., Piscataway 1999, p. 149.

[14] LOUKAS, D.—HARALABIDIS, N.—PAVLIDIS, A.—KARVELAS, E.—PSYCHARIS, V.—MISIAKOS, K.—MOUSA, J.—DRE, Ch.: NIM **A** (2000), in print.

Received 30 October 1999